

Simple human-structure interaction model of walking on a flexible surface

B. Blachowski¹, **P. Holobut**¹, **A. Ortiz**², **J.M. Caicedo**²

¹ Institute of Fundamental Technological Research, Polish Academy of Sciences,
Pawinskiego 5b, 02-106 Warsaw, Poland
e-mail: bblach@ippt.pan.pl

² University of South Carolina, Department of Civil and Environmental Engineering,
300 Main St. Office B122 Columbia, SC 29208, USA

Abstract

We present a new human-structure interaction (HSI) model of walking on a flexible surface. A human is considered as a mass point, located at the body's center of mass (COM). The mass moves along a predefined trajectory, which deforms together with the surface on which the human walks. The forces of motion, equal to the sum of inertial and gravitational forces acting on the mass, are transferred to the surface at prescribed foot positions. The motion of the surface is described using a few selected mode shapes, corresponding damping ratios, and natural frequencies. The equations of motion of the system are time-dependent and discontinuous. They can be written in the form of the second order differential equations of structural dynamics, but with the right-hand forcing dependent on the deformation of the surface. We present a numerical example of a human walking on a long beam structure. The motion of the beam is described by three mode shapes, representing its vertical, lateral, and torsional deflections.

1 Introduction

The last two decades saw increased interest in the dynamical behavior of structures, partly because of the widespread use of numerical computing. Footbridges in particular, which are usually light and flexible structures, present dynamical problems important from both the scientific and the practical points of view. Examples include the Millennium Bridge in London [1] and the Solferino Bridge in Paris [2].

Different explanations of excessive lateral vibrations of footbridges appear in the literature. Fujino [3] pointed out that they are caused by a group of pedestrians synchronizing their movement with the lateral motion of the bridge. In his research, this phenomenon was recorded by a video camera. Another explanation was offered by Blekherman [4], who claims that the reason for excessive lateral vibration is autoparametric resonance. Such a resonance can occur when the ratio between the vertical and the lateral frequency is 2, in which case a coupling between these two modes of vibration takes place. Macdonald [5], however, disagrees with this hypothesis and shows in his paper that the reason for the lateral vibration problems in footbridges lies in the equilibrium of a walking person, who acts on the bridge like a negative damper. Therefore, a sufficiently large group of people can create a negative damping higher than the positive structural damping, which results in large oscillations.

Brownjohn [6] presented a comprehensive study of a vibration response of a suspension footbridge located at a tourist attraction in Singapore. Both continuous and discretized equations were employed to represent the bridge, the latter of which were based on the finite element method. The author presented experimental modal characteristics of the structure, followed by a comparison between numerical simulation and experimental testing. However, the paper uses a 2D model in which only the vertical behavior of the bridge is taken into

consideration.

To predict a vibration response of a footbridge, an appropriate model of the loading is needed in addition to the dynamic characteristics of the structure. In the modeling of a load moving on a bridge, one possible approach is to extend the system matrices (mass, damping, and stiffness) to a form which contains the properties of the moving load, e.g., the size and velocity of the moving mass. In this approach, as exemplified by Filho [7], the stiffness matrix becomes unsymmetric and special solvers are needed to determine the response using the resulting equations of motion. This approach has been applied to the case of a vehicle moving on a bridge, but it can be extended to a pedestrian walking on a footbridge as it was shown by Blachowski et al. [8].

In other papers, pedestrians were assumed to be walking on a rigid surface and then the forces and moments in human joints and muscles were sought. A mathematical model of human locomotion is presented in the paper by Onyshko and Winter [9]. This approach is quite complicated, particularly if the interaction with a moving footbridge deck is included. Nonetheless, a simplified 2D motion has been employed to analyze the interaction between human movement and the lateral vibration of footbridges [10].

Seeking to develop simple methods for predicting dynamic responses of flexible footbridges, Willford and Young [11] first classified footbridges into two groups: low-frequency and high-frequency structures. The limit between these groups was set at 10 Hz for the first natural frequency of the structures. Transient response is considered for high-frequency structures, whereas resonant response is considered for low-frequency structures.

Eurocode [12] provides guidelines for practicing engineers on the design of footbridges, recommending either deterministic or probabilistic methods based on a crowd density parameter for the prediction of dynamic responses of footbridges. Both methods, according to Eurocode, are simple and suitable for practical implementation, but give only an approximate characteristic of the in-service response of a structure.

A reasonable trade-off between computational effort and accuracy was proposed by Kim et al. [13]. In this paper, the loading function caused by a walking pedestrian was represented by a Fourier series. Subsequently, the model was improved by introducing the mass of a walking person and a correction of the loading function due to the moving footbridge deck. Another approach to human-structure interaction was presented by Ortiz Lasprilla et al. [14]. The authors replaced a mass-spring system, which represented human body dynamics, with a PID controller with uncertain parameters.

This paper presents a new HSI model of a human walking on a flexible surface. The working of the model is demonstrated using a numerical example of a human walking over a long beam structure. The motion of the beam is described by three mode shapes, representing vertical, lateral and torsional deflections of the beam. The paper is organized as follows. In Section 2, the proposed HSI model is presented. This section is divided into two subsections: the first one addressing walking on a rigid surface, and the second one extending the approach to the case of a flexible surface. In Section 3, the results of a numerical simulation are presented. Finally, Section 4 discusses the most important defects and limitations of the model.

2 The proposed model of Human-Structure Interaction

We consider a human walking over an elastic structure, which deforms under their weight. The construction of a HSI model consists of building a dynamical model of a structure, a dynamical model of a human, and coupling the two for the walking phase. In our case, the dynamical model of a structure has the form of the standard second-order differential equations of structural dynamics, expressed in modal coordinates. A particular structure is described by a set of selected mode shapes, natural frequencies and damping coefficients, as will be described in Section 2.2. The dynamical model of a walker, and its coupling with the structure, are of a different nature. We assume that the human's COM follows a prescribed trajectory, defined with respect to the structure and deforming together with it. This renders human dynamics dependent on the deformation of the structure. The force of gravity and the forces of inertia resulting from the movement of the COM along

the deformed trajectory are applied to the structure's surface at prescribed foot positions. These forces enter the structure's equations of motion as the right-hand-side loading. This gives the backwards influence of the human motion on the deformation of the structure, and the model is complete. The main assumptions are:

1. The human can be adequately represented as a mass point, placed at their center of mass and having 3 translational degrees of freedom in 3 orthogonal directions.
2. The trajectory of the COM, corresponding to the human walking on a rigid (undeformable) surface, is known. When the human walks on a flexible surface, the prescribed trajectory (locally) deforms together with the surface. This is explained in detail in Section 2.2.
3. In the swing and sway phase of walking, one foot is always in contact with the moving surface regardless of the surface's acceleration—the supporting foot is “attached” to the surface.
4. The phase of walking when the human is supported on both legs is negligibly short.
5. The position of the supporting foot is prescribed as a jump function of time. The movement of the surface does not influence the placement of the foot on the surface.

Some of the above assumptions might not match to what physically occurs experimentally, as discussed at greater length in Section 4. However, they provide a starting point to propose the current methodology, amenable to further changes and improvement.

In the remainder of this section, we present the details of the model and derive its equations of motion. In Section 2.1, we discuss walking on a rigid surface from the perspective of the proposed model. The problem reduces to choosing an appropriate trajectory of the COM over an inflexible surface, further referred to as the *reference trajectory*, and the placement of the supporting foot on the ground—both are parametric functions of time. We present a simple form of approximate trajectory functions, used later in the numerical simulations of Section 3. Then, in Section 2.2, we derive the complete equations of motion of the HSI model for the target case of a flexible surface.

2.1 Walking on a rigid surface

When a human walks on a rigid surface, there is no dynamics of the structure itself and therefore no coupling between the movement of the surface and the movement of the human. Everything reduces to the dynamics of human walking—described, within the present setting, by the trajectory of the COM and the time-dependent placement of the supporting foot. This is schematically illustrated in Figures 1 and 2, where $\mathbf{x}_r(t)$ is the position of the COM at time t , \mathbf{r}_i is the position of some reference point of the supporting foot during the i -th step, $t_i \leq t < t_{i+1}$, and $\mathbf{s}(t)$ is the point at which the ground reaction force (GRF) at time t is applied (center of pressure of the supporting foot). In general, $\mathbf{r}_i \neq \mathbf{s}(t)$, but $\mathbf{s}(t)$ must lie within the supporting foot's area to allow the foot to actually support the COM.

In the case when experimental data on a COM's motion are available, one can generate real-life walking trajectories and input them to the HSI model. Otherwise, theoretical trajectories may be used as an approximation. For the purpose of this paper, construction of a real-life trajectory based on experimental data is not attempted. We use simple functions which possess qualitative characteristics of real walking, and give reasonable quantitative approximations to a mechanically-balanced gait. In particular, for some portions of the trajectories, $\mathbf{s}(t)$ will lie farther away from \mathbf{r}_i than required by the foot size. Such shortcomings may be corrected, if necessary, by including the double-support phase of walking and further adjustment of the trajectory functions.

Figure 2 shows a side view (top) and top view (middle) of a typical trajectory of the COM, plus a corresponding longitudinal velocity (bottom). The vertical position of the COM, $z_r(t)$, its lateral position, $y_r(t)$, and its velocity $v(t) = \dot{x}_r(t)$ are described by three in-phase periodic functions, where the period of $y_r(t)$ is

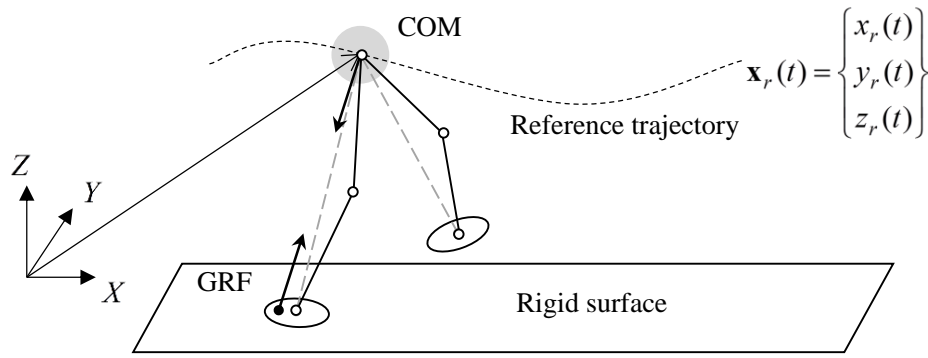


Figure 1: Trajectory of a human’s COM, and the GRF, during walking on a rigid surface.

twice the period of $z_r(t)$ and $\dot{x}_r(t)$. The lowest point of $z_r(t)$ corresponds to the moment of change of the supporting foot, and the highest—to the vertical position of the supporting leg. The velocity $\dot{x}_r(t)$ is lowest when the supporting leg is in the vertical position, and highest at the change of the supporting foot.

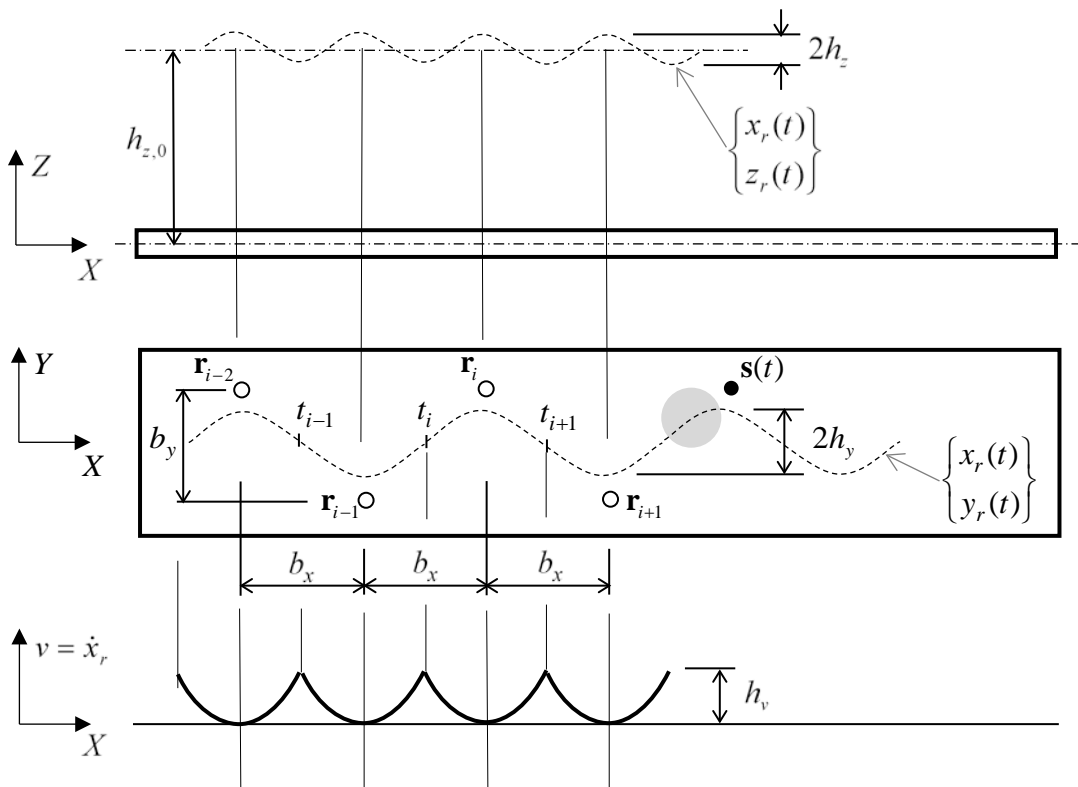


Figure 2: Walking path over a rigid surface: vertical path of the COM (top), lateral path of the COM and supporting foot’s positions (middle), and the COM’s longitudinal velocity (bottom).

In the simulations of Section 3, we use the following description of the trajectory of the COM and supporting foot’s locations.

1. The assumed walking parameters are: step length b_x , lateral sway amplitude h_y , vertical sway amplitude h_z , mean vertical position $h_{z,0}$, mean horizontal position $h_{y,0}$, maximum longitudinal velocity v_0 , and maximum range of longitudinal velocity h_v . The parameters should be adjusted to generate a dynamically feasible trajectory.

2. The longitudinal velocity of the COM is assumed to be

$$\dot{x}_r(t) = v(t) = v_0 - |h_v \sin(ft)| \tag{1}$$

where the frequency f is obtained from the identity $\int_0^{\pi/f} v(t)dt = b_x$, which gives

$$f = \frac{v_0\pi - 2h_v}{b_x} \tag{2}$$

3. The longitudinal position of the COM at time t is obtained by integrating $v(t)$:

$$x_r(t) = \int_0^t v(\tau)d\tau = v_0t - \frac{h_v}{f} \left(2 \left\lfloor \frac{ft}{\pi} \right\rfloor + 1 - \cos(ft \bmod \pi) \right) \tag{3}$$

4. The lateral and vertical components of the trajectory are assumed to be

$$y_r(t) = h_{y,0} + h_y \sin\left(\frac{\pi}{b_x} x_r(t)\right) \tag{4}$$

$$z_r(t) = h_{z,0} - h_z \cos\left(\frac{2\pi}{b_x} x_r(t)\right) \tag{5}$$

5. The reference positions of the supporting foot, \mathbf{r}_i , are chosen in such a way as to best approximate the positions of the GRFs resulting from the movement of the COM along $\mathbf{x}_r(t)$. Therefore \mathbf{r}_i are the outcome of $\mathbf{x}_r(t)$.

Figure 3 presents GRFs corresponding to one step cycle of an example COM’s trajectory of the above type. Each arrow represents a scaled GRF. The tails of most arrows are concentrated around supporting foot’s positions, as is required by real walking dynamics. Exceptions are GRFs corresponding to the portions of the trajectory near the change of the supporting foot. The inclusion of a double-support phase of walking might largely resolve this issue.

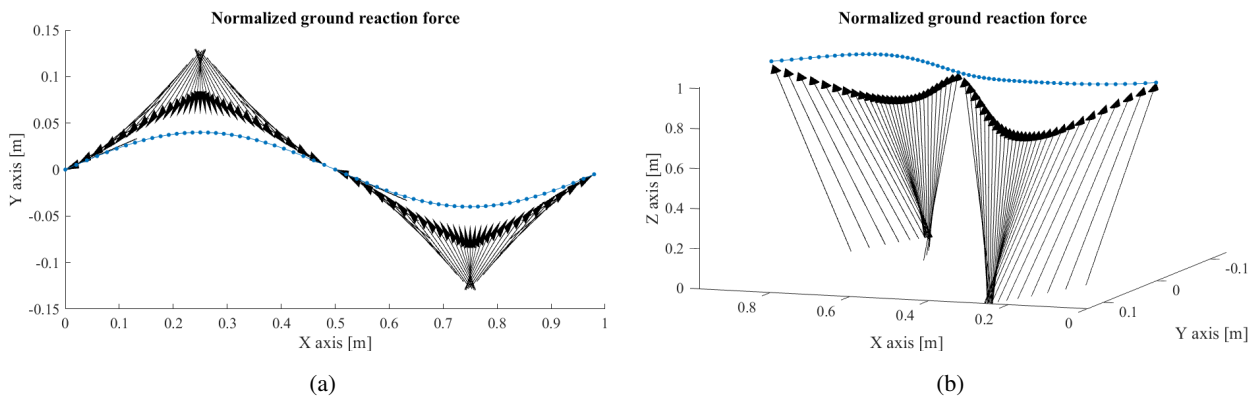


Figure 3: GRFs for a typical COM’s trajectory of the proposed type: top view (a) and 3D view (b). The arrows are normalized so that the length of the longest is 1.

2.2 Walking on a deformable surface

It is assumed that human motion control is performed in such a way that the position of the COM with respect to the moving surface is the same as it would be with respect to the rigid surface at the same time t . When the prescribed trajectory of the COM deforms with the surface, this condition is satisfied.

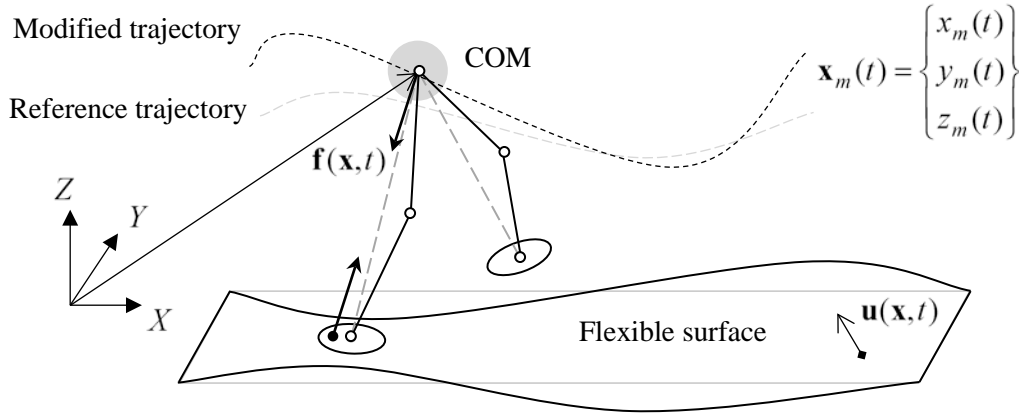


Figure 4: Trajectory of a human's COM during walking on a deformable surface.

Using the above assumption and the notation presented in Figure 4, one can decompose the trajectory of the COM on a deformable surface as follows:

$$\mathbf{x}_m(t) = \mathbf{x}_r(t) + \mathbf{u}(\mathbf{x}_s, t) \quad (6)$$

where \mathbf{x}_r represents the reference trajectory of the COM (walking on a rigid surface), and $\mathbf{u}(\mathbf{x}_s, t)$ is the displacement vector of the deformable surface at location $\mathbf{x}_s = [x_r(t), y_r(t)]^T$ and time t .

We assume that the motion of the deformable surface can be described using a set of n_m modes, and corresponding damping ratios and natural frequencies. Therefore the vector of displacement can be written in the form

$$\mathbf{u}(\mathbf{x}_s, t) = \Phi(\mathbf{x}_s)\boldsymbol{\eta}(t) \quad (7)$$

where $\Phi(\mathbf{x}_s) = [\phi^{(1)}(\mathbf{x}_s), \phi^{(2)}(\mathbf{x}_s), \dots, \phi^{(n_m)}(\mathbf{x}_s)]$ is a matrix composed of mode-shape functions and $\boldsymbol{\eta}(t) = [\eta_1(t), \eta_2(t), \dots, \eta_{n_m}(t)]^T$ is a vector of modal amplitudes, or in the equivalent form:

$$\mathbf{u}(\mathbf{x}_s, t) = \sum_{i=1}^{n_m} \phi^{(i)}(\mathbf{x}_s)\eta_i(t) = \sum_{i=1}^{n_m} \begin{bmatrix} \phi_x(\mathbf{x}_s) \\ \phi_y(\mathbf{x}_s) \\ \phi_z(\mathbf{x}_s) \end{bmatrix}^{(i)} \eta_i(t) \quad (8)$$

We shall assume, as an approximation, that the force exerted on the surface by the walker is applied not at the center of pressure, but at the reference position of the foot \mathbf{r}_i . The force exerted on the surface is therefore

$$\mathbf{f}(\mathbf{x} = \mathbf{r}_i, t \in [t_i, t_{i+1})) = -m\ddot{\mathbf{x}}_m(t) + m\mathbf{g} \quad (9)$$

where $\mathbf{r}_i = [r_{i,x}, r_{i,y}]^T$ is a vector representing the location of the foot on the surface during the i -th step, m is the mass of the human, and \mathbf{g} is the vector of gravitational acceleration. Eq. (9) should be treated as the first approximation to the interaction between the mass and the surface. It simply describes the transfer to the surface, at an approximate position, of the forces of gravity and inertia acting on the mass along the trajectory. The resulting motion is not dynamically well-balanced, because the position at which the force is applied to the surface is not exact.

The differentiation in Eq. (9) has to be performed keeping in mind that \mathbf{x}_s , which appears in Eqs. (6), (7) and (8), is time-dependent. One obtains

$$\dot{\mathbf{x}}_m = \dot{\mathbf{x}}_r + \frac{d}{dt} \left(\sum_{i=1}^{n_m} \phi^{(i)}(\mathbf{x}_s)\eta_i(t) \right) = \dot{\mathbf{x}}_r + \sum_{i=1}^{n_m} \left(\frac{\partial \phi^{(i)}}{\partial \mathbf{x}} \dot{\mathbf{x}}_s \eta_i(t) + \phi^{(i)}(\mathbf{x}_s) \dot{\eta}_i(t) \right) \quad (10)$$

$$\ddot{\mathbf{x}}_m = \ddot{\mathbf{x}}_r + \sum_{i=1}^{n_m} \left[\left(\dot{\mathbf{x}}_s^T \frac{\partial^2 \phi^{(i)}}{\partial \mathbf{x}^2} \dot{\mathbf{x}}_s + \frac{\partial \phi^{(i)}}{\partial \mathbf{x}} \ddot{\mathbf{x}}_s \right) \eta_i(t) + 2 \frac{\partial \phi^{(i)}}{\partial \mathbf{x}} \dot{\mathbf{x}}_s \dot{\eta}_i(t) + \phi^{(i)}(\mathbf{x}_s) \ddot{\eta}_i(t) \right] \quad (11)$$

Additional information about the matrices in Eqs. (10) and (11) is provided in Appendix A.

The resulting, combined dynamical system (human dynamics + dynamics of a flexible structure) is time-dependent and discontinuous. Its equations of motion can be written in the form which is well known in structural dynamics, but with the left hand side vector dependent on the current deformation of the structure

$$\ddot{\boldsymbol{\eta}} + 2\mathbf{Z}\boldsymbol{\Omega}\dot{\boldsymbol{\eta}} + \boldsymbol{\Omega}^2\boldsymbol{\eta} = \mathbf{B}_i\mathbf{f}(\boldsymbol{\eta}, \dot{\boldsymbol{\eta}}, \ddot{\boldsymbol{\eta}}, t), \quad t \in [t_i, t_{i+1}), \quad i = 0, 1, 2, \dots \quad (12)$$

where $\mathbf{Z} = \text{diag}(\zeta_1, \zeta_2, \dots, \zeta_{n_m})$, $\boldsymbol{\Omega} = \text{diag}(\omega_1, \omega_2, \dots, \omega_{n_m})$, \mathbf{B}_i is the influence matrix for the force \mathbf{f} acting at position \mathbf{r}_i on the surface, and \mathbf{f} is defined by Eq. (9). If one rewrites Eq. (11) in the form

$$\ddot{\mathbf{x}}_m = \mathbf{f}_r(\boldsymbol{\eta}, \dot{\boldsymbol{\eta}}, t) + \boldsymbol{\Phi}(\mathbf{x}_s)\ddot{\boldsymbol{\eta}} \quad (13)$$

then, after substituting Eq. (13) into Eq. (9), the result into Eq. (12), and solving for $\ddot{\boldsymbol{\eta}}$, one finally obtains

$$\ddot{\boldsymbol{\eta}} = [\mathbf{I} + m\mathbf{B}_i\boldsymbol{\Phi}(\mathbf{x}_s)]^{-1}[m\mathbf{B}_i(\mathbf{g} - \mathbf{f}_r(\boldsymbol{\eta}, \dot{\boldsymbol{\eta}}, t)) - 2\mathbf{Z}\boldsymbol{\Omega}\dot{\boldsymbol{\eta}} - \boldsymbol{\Omega}^2\boldsymbol{\eta}] \quad (14)$$

Eq. (14) is the basis for the numerical simulations of Section 3.

3 Numerical simulations

As an example of human-structure interaction, we analyze below a human walking over a long beam-like structure. It is assumed that the motion of the beam can be described using three mode shapes representing vertical, lateral and torsional deflections of the beam—as shown in Figure 5. The advantage of the approach is that it is not necessary to build a Finite Element model of the structure under consideration. In practice, any technique allowing to obtain even approximate mode shapes and corresponding natural frequencies of a structure can be used.

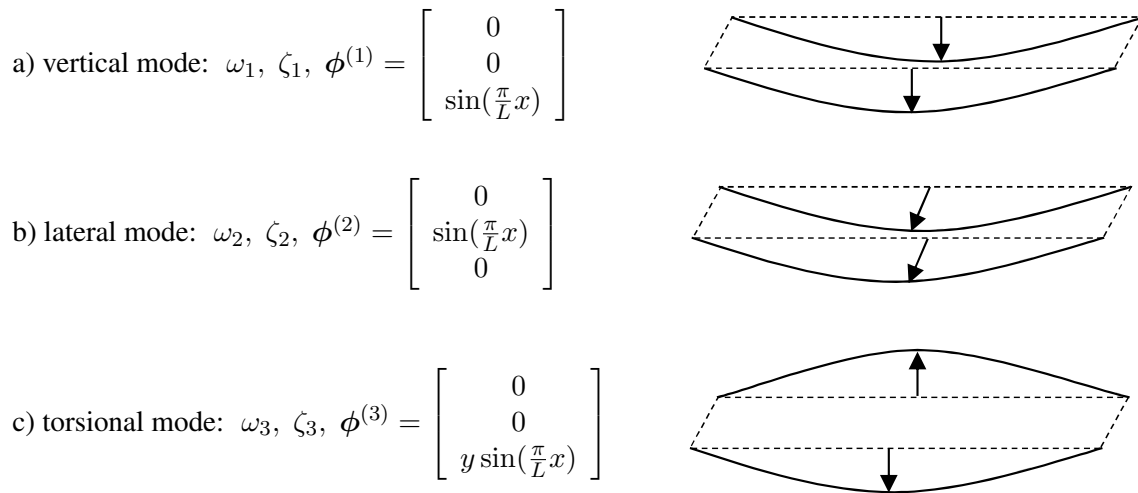


Figure 5: Mode characteristics of the flexible surface.

Assuming small deformations and using the three modes shown in Figure 5, the displacement vector can be written as

$$\mathbf{u}(\mathbf{x}, t) = \begin{bmatrix} 0 \\ \sin(\frac{\pi}{L}x)\eta_2(t) \\ \sin(\frac{\pi}{L}x)\eta_1(t) + y \sin(\frac{\pi}{L}x)\eta_3(t) \end{bmatrix} \quad (15)$$

The modal damping and spectral matrices have the form

$$\mathbf{Z} = \begin{bmatrix} \zeta_1 & 0 & 0 \\ 0 & \zeta_2 & 0 \\ 0 & 0 & \zeta_3 \end{bmatrix}, \quad \boldsymbol{\Omega} = \begin{bmatrix} \omega_1 & 0 & 0 \\ 0 & \omega_2 & 0 \\ 0 & 0 & \omega_3 \end{bmatrix} \quad (16)$$

We use the following values of the parameters:

- beam parameters
 $L = 50$ m (length), $W = 4$ m (width), $\rho = 200$ kg/m² (mass per unit area), $\zeta_1 = \zeta_2 = \zeta_3 = 0.005$,
 $\omega_1 = 0.7$ Hz, $\omega_2 = \omega_3 = 1.4$ Hz
- mass of the walker
 $m = 100$ kg
- trajectory parameters
 - trajectory 1 (fast walking): $b_x = 0.9$ m, $b_y = 0.2$ m, $h_{y,0} = 0$ m, $h_y = 0.02$ m, $h_{z,0} = 1$ m, $h_z = 0.02$ m, $v_0 = 2$ m/s, $h_v = 0.5$ m/s
 - trajectory 2 (moderate walking): $b_x = 0.7$ m, $b_y = 0.22$ m, $h_{y,0} = 0$ m, $h_y = 0.03$ m, $h_{z,0} = 1$ m, $h_z = 0.015$ m, $v_0 = 1.5$ m/s, $h_v = 0.4$ m/s
 - trajectory 3 (slow walking): $b_x = 0.5$ m, $b_y = 0.26$ m, $h_{y,0} = 0$ m, $h_y = 0.04$ m, $h_{z,0} = 1$ m, $h_z = 0.01$ m, $v_0 = 1$ m/s, $h_v = 0.3$ m/s

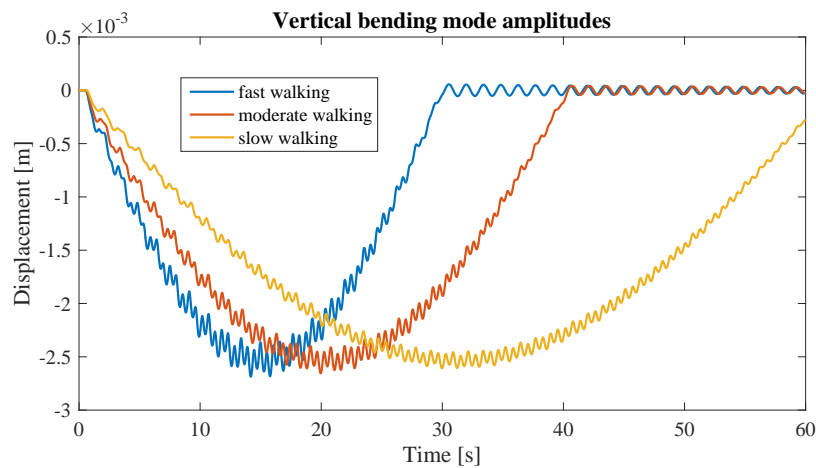


Figure 6: Values of $\eta_1(t)$ during the passage of the walker over the beam, for the three COM's trajectories.

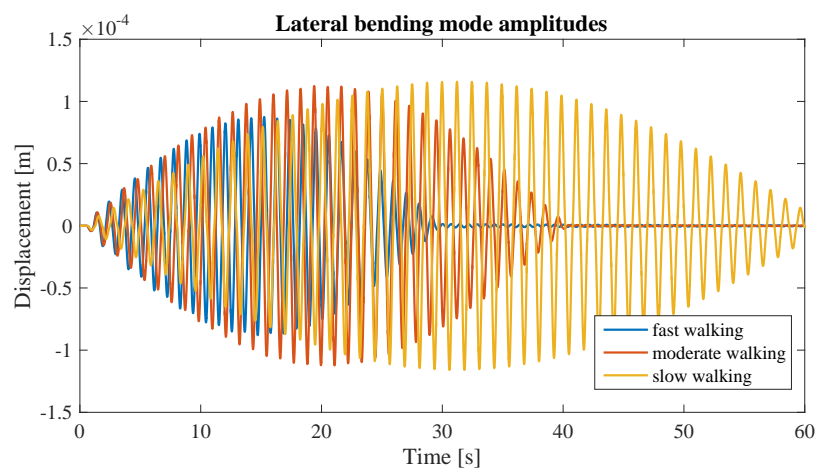


Figure 7: Values of $\eta_2(t)$ during the passage of the walker over the beam, for the three COM's trajectories.

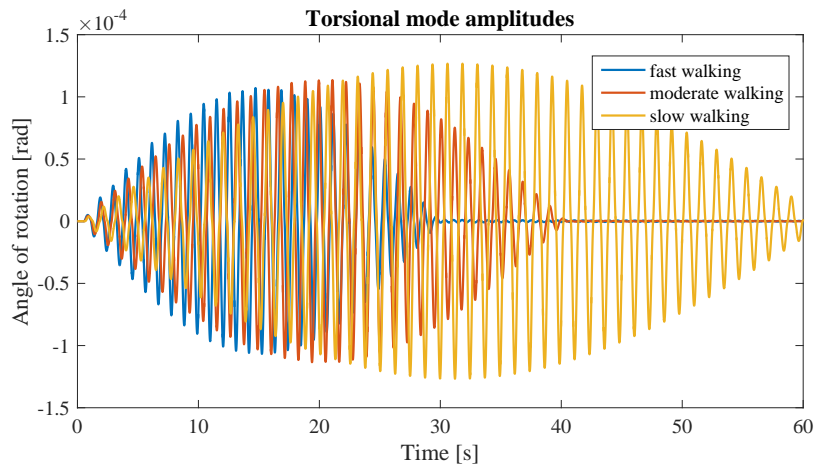


Figure 8: Values of $\eta_3(t)$ during the passage of the walker over the beam, for the three COM's trajectories.

The results are shown in Figures 6, 7, and 8. One can observe in Figure 6 that faster walking induces larger vibrations of the vertical mode, mainly because of greater amplitudes of the vertical motion of the COM during faster walking. Conversely, the fastest walk induces the smallest vibrations of the lateral and torsional modes, as can be seen in Figures 7 and 8. This may be related to the increased amplitude of the lateral sway of the COM during slower walking. Also, it can be observed in Figure 6 that, because of the low value of ω_1 , a more complex vibrational response of the 1st mode occurs.

4 Discussion and conclusions

We proposed a new HSI model of walking on a flexible surface. The predictions possess qualitative features expected of the dynamics of human-structure interaction. We therefore expect that the present model will be a good starting point for developing more accurate HSI models.

The main advantage of the model is its relative simplicity. The model does not involve complex human dynamics. It also uses a simple, mode-shape based model of a structure, and therefore does not require extensive FEM computations. To obtain the structural response one needs to numerically integrate a system of ordinary differential equations with several degrees of freedom—the simulations of Section 3 took a few seconds on a desktop PC.

There are also several obvious drawbacks of the present model which indicate directions for further development. We discuss them briefly below.

1. The proposed trajectories of the COM, as described in Section 2.1 and used in the simulations, do not accurately represent real human COM's motion. Most conspicuously, for some fragments of the trajectories, the GRFs are located away from the assumed supporting foot's positions. To yield a dynamically balanced motion, the reaction forces would have to be much more concentrated so that all GRFs fall within the supporting foot's area. As it was mentioned earlier, the inclusion of the double-support phase of walking and a better adjustment of the trajectory functions would solve this issue.
2. The model expressed by Eqs. (12) and (14) applies the GRF at the supporting foot's reference position \mathbf{r}_i . In reality, the force should be applied at the time-dependent $\mathbf{s}(t)$, which in general differs from \mathbf{r}_i . As a result, \mathbf{B}_i would not be constant in the course of one step, but would turn into a state-dependent $\mathbf{B}(\boldsymbol{\eta}, \dot{\boldsymbol{\eta}}, \ddot{\boldsymbol{\eta}}, t)$. It would no longer be possible to explicitly solve Eq. (12) for $\ddot{\boldsymbol{\eta}}$ as in Eq. (14). Numerical solutions would be necessary, increasing the computational burden of the procedure.

3. Deformation of $\mathbf{x}_r(t)$ during deformation of the structure, as described by Eq. (6), may not accurately capture real motion of the COM. This, of course, depends to some degree on the particular walking person, their physical capabilities and walking objectives. Nonetheless, it may be presumed that the lateral movement of the COM is less correlated with the lateral movement of the structure than are the corresponding vertical movements. Also, the deformation of the trajectory should be related with the displacement of the structure at \mathbf{r}_i rather than at $\mathbf{x}_s(t)$. Both of these matters should be accounted for in a more precise model.
4. During large vibrations of the structure, the GRFs resulting from even a well-chosen reference trajectory of the COM may fall outside the area of the supporting foot. In such a case, a formulation of walking objectives and feedback control of the COM's movement may be needed to replace the simple approach of the present paper.

Acknowledgements

The first author wishes to express his gratitude for the financial support provided by the National Science Centre, Poland (0494/B/T02/2011/40).

References

- [1] S.H. Strogatz, D.M. Abrams, A. McRobbie, B. Eckhard, E. Ott, *Crowd synchrony on the Millennium Bridge*, Nature, Vol. 438, No. 3, (2005), pp. 43-44.
- [2] A.N. Blekherman, *Autoparametric resonance in a pedestrian steel arch bridge: Solferino Bridge, Paris*, ASCE Journal of Bridge Engineering, Vol. 12, No. 6, (2007), pp. 669-676.
- [3] Y. Fujino, B.M. Pacheco, S. Nakamura, P. Warnichai, *Synchronization of human walking observed during lateral vibration of a congested pedestrian bridge*, Earthquake Engineering & Structural Dynamics, Vol. 22, No. 9, (1993), pp. 741-758.
- [4] A.N. Blekherman, *Swaying of pedestrian bridges*, Journal of Bridge Engineering, Vol. 10, No. 2, (2005), pp. 142-150.
- [5] J.H.G. Macdonald, *Lateral excitation of bridges by balancing pedestrians*, Proceedings of the Royal Society A, Vol. 465, No. 2104, (2009), pp. 1055-1073.
- [6] J.M.W. Brownjohn, *Vibration characteristics of a suspension footbridge*, Journal of Sound and Vibration, Vol. 202, No. 1, (1998), pp. 29-46.
- [7] F.V. Filho, *Finite element analysis of structures under moving loads*, The Shock and Vibration Digest, Vol. 10, No. 8, (1978), pp. 27-35.
- [8] B. Blachowski, W. Gutkowski, P. Wisniewski, *Dynamic Substructuring Approach for Human Induced Vibration of a Suspension Footbridge*, in *Proceedings of PCM-CMM 2015—3rd Polish Congress of Mechanics & 21st Computer Methods in Mechanics*, (2015), pp. 307-308.
- [9] S. Onyshko, D.A. Winter, *A mathematical model for the dynamics of human locomotion*, Journal of Biomechanics, Vol. 13, No. 4, (1980), pp. 361-368.
- [10] M. Bocian, J.H.G. Macdonald, J.F. Burn, *Biomechanically inspired modeling of pedestrian-induced forces on laterally oscillating structures*, Journal of Sound and Vibration, Vol. 331, No. 16, (2012), pp. 3914-3929.

-
- [11] M. Willford, P. Young, *A Design Guide for Footfall Induced Vibration of Structures*, The Concrete Center (2006).
- [12] Ch. Heinemeyer, Ch. Butz, A. Keil, M. Schlaich, A. Goldack, S. Trometer, M. Lukic, B. Chabrolin, A. Lemaire, P.O. Martin, A. Cunha, E. Caetano, *Design of Lightweight Footbridges for Human Induced Vibrations*, JRC Scientific and Technical Reports (2009).
- [13] S.H. Kim, K.I. Cho, M.S. Choi, J.Y. Lim, *Development of human body model for the dynamic analysis of footbridges under pedestrian induced excitation*, *Steel Structures*, Vol. 8, (2008), pp. 333-345.
- [14] A.R. Ortiz Lasprilla, J.M. Caicedo, G.A. Ospina, *Modeling Human-Structure Interaction Using a Close Loop Control System*, *Dynamics of Civil Structures*, Vol. 4, *Proceedings of the 32nd IMAC—A Conference and Exposition on Structural Dynamics*, (2014), pp 101-108.

A Details of the equations of motion

To perform numerical simulations using Eq. (14), the following vectors and matrices have to be determined.

1. The first derivative of the COM's trajectory with respect to time:

$$\dot{\mathbf{x}}_s = \begin{bmatrix} \dot{x}_r(t) \\ y_{r,x}\dot{x}_r(t) \end{bmatrix} \quad (17)$$

where

$$y_{r,x} = \frac{\partial y_r}{\partial x} \quad (18)$$

2. The second derivative of the COM's trajectory with respect to time:

$$\ddot{\mathbf{x}}_s = \begin{bmatrix} \ddot{x}_r(t) \\ y_{r,xx}\dot{x}_r^2(t) + y_{r,x}\ddot{x}_r(t) \end{bmatrix} \quad (19)$$

3. The first derivative of the i -th mode shape with respect to spatial coordinates:

$$\frac{\partial \phi^{(i)}}{\partial \mathbf{x}} = \begin{bmatrix} \phi_{x,x} & \phi_{x,y} \\ \phi_{y,x} & \phi_{y,y} \\ \phi_{z,x} & \phi_{z,y} \end{bmatrix}^{(i)} \quad (20)$$

4. The second derivative of the i -th mode shape with respect to spatial coordinates:

$$\frac{\partial^2 \phi^{(i)}}{\partial \mathbf{x}^2} = \left[\frac{\partial^2 \phi_x^{(i)}}{\partial \mathbf{x}^2} \mid \frac{\partial^2 \phi_y^{(i)}}{\partial \mathbf{x}^2} \mid \frac{\partial^2 \phi_z^{(i)}}{\partial \mathbf{x}^2} \right] \quad (21)$$

where

$$\frac{\partial^2 \phi_x^{(i)}}{\partial \mathbf{x}^2} = \begin{bmatrix} \phi_{x,xx} & \phi_{x,xy} \\ \phi_{x,xy} & \phi_{x,yy} \end{bmatrix}^{(i)} \quad (22)$$

$$\frac{\partial^2 \phi_y^{(i)}}{\partial \mathbf{x}^2} = \begin{bmatrix} \phi_{y,xx} & \phi_{y,xy} \\ \phi_{y,xy} & \phi_{y,yy} \end{bmatrix}^{(i)} \quad (23)$$

$$\frac{\partial^2 \phi_z^{(i)}}{\partial \mathbf{x}^2} = \begin{bmatrix} \phi_{z,xx} & \phi_{z,xy} \\ \phi_{z,xy} & \phi_{z,yy} \end{bmatrix}^{(i)} \quad (24)$$